

University of Nebraska - Lincoln

DigitalCommons@University of Nebraska - Lincoln

Xiao Cheng Zeng Publications

Published Research - Department of Chemistry

4-21-2008

Search for lowest-energy structure of Zintl dianion Si_{12}^{2-} , Ge_{12}^{2-} , and Sn_{12}^{2-}

Nan Shao

University of Nebraska-Lincoln

Satya S. Bulusu

University of Nebraska-Lincoln, sbulusu@iiti.ac.in

Xiao Cheng Zeng

University of Nebraska-Lincoln, xzeng1@unl.edu

Follow this and additional works at: <https://digitalcommons.unl.edu/chemzeng>

 Part of the [Chemistry Commons](#)

Shao, Nan; Bulusu, Satya S.; and Zeng, Xiao Cheng, "Search for lowest-energy structure of Zintl dianion Si_{12}^{2-} , Ge_{12}^{2-} , and Sn_{12}^{2-} " (2008). *Xiao Cheng Zeng Publications*. 85.

<https://digitalcommons.unl.edu/chemzeng/85>

This Article is brought to you for free and open access by the Published Research - Department of Chemistry at DigitalCommons@University of Nebraska - Lincoln. It has been accepted for inclusion in Xiao Cheng Zeng Publications by an authorized administrator of DigitalCommons@University of Nebraska - Lincoln.

Search for lowest-energy structure of Zintl dianion Si_{12}^{2-} , Ge_{12}^{2-} , and Sn_{12}^{2-}

Nan Shao, Satya Bulusu, and X. C. Zeng^{a)}

Department of Chemistry, University of Nebraska-Lincoln Lincoln, Nebraska 68588, USA

(Received 16 January 2008; accepted 22 February 2008; published online 21 April 2008)

We perform an unbiased search for the lowest-energy structures of Zintl dianions (Si_{12}^{2-} , Ge_{12}^{2-} , and Sn_{12}^{2-}), by using the basin-hopping (BH) global optimization method combined with density functional theory geometric optimization. High-level *ab initio* calculation at the coupled-cluster level is used to determine relative stabilities and energy ranking among competitive low-lying isomers of the dianions obtained from the BH search. For Si_{12}^{2-} , all BH searches (based on independent initial structures) lead to the same lowest-energy structure Si_{12a}^{2-} , a tricapped trigonal prism (TTP) with C_{3v} group symmetry. Coupled-cluster calculation, however, suggests that another TTP isomer of Si_{12c}^{2-} is nearly isoenergetic with Si_{12a}^{2-} . For Sn_{12}^{2-} , all BH searches lead to the icosahedral structure $I_h\text{-Sn}_{12a}^{2-}$, i.e., the *stannaspherene*. For Ge_{12}^{2-} , however, most BH searches lead to the TTP-containing Ge_{12b}^{2-} , while a few BH searches lead to the empty-cage icosahedral structure $I_h\text{-Ge}_{12a}^{2-}$ (named as *germaniaspherene*). High-level *ab initio* calculation indicates that $I_h\text{-Ge}_{12a}^{2-}$ and TTP-containing Ge_{12b}^{2-} are almost isoenergetic and, thus, both may be considered as candidates for the lowest-energy structure at 0 K. Ge_{12a}^{2-} has a much larger energy gap (2.04 eV) between highest occupied molecular orbital and lowest unoccupied molecular orbital than Ge_{12b}^{2-} (1.29 eV), while Ge_{12b}^{2-} has a lower free energy than $I_h\text{-Ge}_{12a}^{2-}$ at elevated temperature (>980 K). The TTP-containing Si_{12a}^{2-} and Ge_{12b}^{2-} exhibit large negative nuclear independent chemical shift (NICS) value (~ -44) at the center of TTP, indicating aromatic character. In contrast, germaniaspherene $I_h\text{-Ge}_{12a}^{2-}$ and stannaspherene $I_h\text{-Sn}_{12a}^{2-}$ exhibit modest positive NICS values, ~ 12 and 3, respectively, at the center of the empty cage, indicating weakly antiaromatic character. © 2008 American Institute of Physics. [DOI: 10.1063/1.2897918]

I. INTRODUCTION

Although group-14 Zintl ion clusters can be described by substituting a B–H unit of deltahedral boranes with group-14 atoms,¹ the aromaticity of borane dianion $\text{B}_n\text{H}_n^{2-}$ may be quite different from that of Zintl dianions E_n^{2-} (E = Si, Ge, Sn, Pb). $\text{B}_n\text{H}_n^{2-}$ ($4 < n < 13$) generally exhibit diatropic nuclear independent chemical shift (NICS) at their polyhedron center. For example, the isoelectronic $I_h\text{-B}_{12}\text{H}_{12}^{2-}$ is highly aromatic with a negative NICS value of ~ -27 at the cage center. In contrast, icosahedral $I_h\text{-Si}_{12}^{2-}$ exhibits a paratropic NICS value (56.4) at the cage center, a characteristic of antiaromaticity. King *et al.* attributed this antiaromaticity to the very paratropic threefold degenerate t_{1u} and the fivefold degenerate h_g molecular orbitals (MOs) of $I_h\text{-Si}_{12}^{2-}$ that offset the diatropicity.² The difference in aromaticity between magic clusters Si_6^{2-} and Si_7^{2-} with the corresponding isoelectronic boranes has been recently demonstrated by Zdzetsis.³


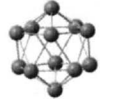
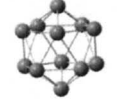





















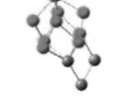
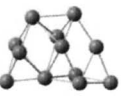



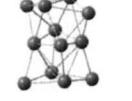
Also, it is known that Wade's $2n+2$ skeletal electron rule for closed polyhedron, derived originally from *closo* carboranes, boranes and borane anions,⁴ can be extended to predicting stability of group-14 E_n^{x-} anions ($x=2-4$). For example, all the dianions E_{12}^{2-} (E = Si, Ge, Sn, Pb) possess 26 skeletal electrons and, thus, should be stable according to the

Wade's rule. Indeed, polyatomic anions of Sn_{12}^{2-} and Pb_{12}^{2-} have recently been synthesized in the laboratory.^{5,6} Since both Sn_{12}^{2-} and Pb_{12}^{2-} exhibit delocalized π bonding character and have empty-cage icosahedral structure, the two clusters are named as *stannaspherene* and *plumbaspherene*, respectively, by Wang and co-workers.^{5,6} In solids, endohedral group-14 dianion units, such as $\text{M}@\text{Pb}_{12}^{2-}$ [M = Ni,⁷ Pd,⁷ and Pt (Ref. 8)], have been shown to have an icosahedral structure by single-crystal x-ray diffraction, energy dispersive x-ray, and NMR spectroscopy experiments. Gas-phase endohedral clusters $\text{M}^{2+}@\text{Sn}_{12}^{2-}$ (M = Ti, V, Cr, Fe, Co, Ni, Cu, Y, Nb, Gd, Hf, Ta, Pt, and Au)⁹ and AlPb_{12}^+ (Ref. 10) have been synthesized in the laboratory. Previous first-principles calculations show that the “outligands” and “intraligands” only weakly interact with the icosahedral cage Pb_{12}^{2-} and Sn_{12}^{2-} .^{5,6,8}

Although the global-minimum structures of Zintl dianion clusters Sn_{12}^{2-} and Pb_{12}^{2-} are fully established, to our knowledge, the global-minimum structures of Si_{12}^{2-} and Ge_{12}^{2-} are still unknown. Chen *et al.* have shown that the empty-cage $I_h\text{-Si}_{12}^{2-}$ is not the global minimum.¹¹ Whether Ge_{12}^{2-} exhibits the same (lowest-energy) icosahedral structure as the stannaspherene Sn_{12}^{2-} or that as the lowest-energy structure of Si_{12}^{2-} is another open question. In this paper, we present results of low-lying structures of group-14 dianionic clusters Si_{12}^{2-} , Ge_{12}^{2-} , and Sn_{12}^{2-} , based on an unbiased global-

^{a)}Electronic mail: xczen@phase2.unl.edu.

TABLE I. Top ten low-lying isomers of Si_{12}^{2-} , Ge_{12}^{2-} , and Sn_{12}^{2-} . The energy rankings are based on PBE/DNP-ECP calculations, while the relative energy shown in parentheses is based on PBEPBE/6-311+G(*d*) calculation, including zero-point energy correction. ΔE is in units of eV. The TTP motif is highlighted in opaque gray.

Index	Si_{12}^{2-}			Ge_{12}^{2-}			Sn_{12}^{2-}		
	ΔE^a	Sym. ^b	Structure	ΔE^a	Sym. ^b	Structure	ΔE^a	Sym. ^b	Structure
a	0.00 (0.000)	C_s		0.00 (0.000)	I_h		0.00	I_h	
b	0.08 (0.158)	C_s		0.26 (0.067)	C_1		0.54	C_1	
c	0.08 (0.078)	C_s		0.27 (0.33)	C_1		0.76	C_1	
d	0.21 (0.423)	S_6		0.36	C_s		0.77	C_s	
e	0.37	C_1		0.47	C_s		0.82	C_2	
f	0.40	C_s		0.48	C_1		0.82	C_1	
g	0.44	C_1		0.49	C_s		0.83	C_s	
h	0.47	C_s		0.51	C_1		0.85	C_1	
i	0.50	C_s		0.53	C_s		0.87	C_s	
j	0.50	C_1		0.54	S_6		0.88	C_2	

^aRelative energies are calculated using DMOL3 program. Medium integration grid and 4.0 Å global cutoff are selected. Relative energies shown in parentheses are calculated using GAUSSIAN 03 package.

^bSymmetry is obtained within a numerical tolerance of 0.1 Å.

minimum search. Electronic and aromatic properties of the low-lying structures of Si_{12}^{2-} and Ge_{12}^{2-} are also presented.

II. COMPUTATIONAL DETAILS

To search for the lowest-energy structures of Zintl dianions E_{12}^{2-} , ($E=\text{Si}$, Ge , and Sn), a three-step computation procedure is undertaken. First, an unbiased search is performed, using the basin-hopping¹² (BH) method combined with density functional theory (DFT) geometric optimiza-

tion. Specifically, the gradient-corrected Perdew–Burke–Ernzerhof (PBE) exchange–correlation functional¹³ and the double-numerical polarized basis set with effective core potential (ECP), implemented in DMOL3 software,¹⁴ are chosen for geometric optimization. The combined DFT–BH approach has been proven to be quite effective to generate a large number of low-energy clusters (typically 200–400 isomers). This approach has been used to search for the global minima of medium-sized boron, germanium, and gold

TABLE II. Point-group symmetries, relative energies (ΔE) (for Si and Ge), HOMO-LUMO gaps, and GIAO-NICSs of Zintl dianions at singlet state. Energies and HOMO-LUMO gaps are in units of eV, zero-point energy (ZPE) in a.u., and NICS in ppm. The lowest-energy isomers are highlighted in boldface.

	Si_{12a}^{2-}	Si_{12b}^{2-}	Si_{12c}^{2-}	Si_{12d}^{2-}	$I_h\text{-Si}_{12}^{2-}$
Structure	TTP	TTP	TTP	Chair	Icos
Symmetry ^a	C_1	C_1	C_1	$C_1(D_{3d}0.1)$	I_h
ΔE [PBEPBE/6-311+G(<i>d</i>)] _{ZPE}	0.000	0.158	0.078	0.423	1.572
ΔE [MP2/6-31+G(<i>d</i>)]	0.000	0.775	0.377	1.285	
ZPE [MP2/6-31+G(<i>d</i>)]	0.0199	0.0195	0.0196	0.0201	
ΔE [MP2/6-311+G(2 <i>d</i>)]	0.000	0.437	0.465	1.720	
ΔE [CCSD(T)/6-311+G(2 <i>d</i>)]	0.031	0.751	0.000	0.500	
HOMO-LUMO gap ^b	1.297	1.420	1.544	1.913	1.601
NICS ^b	-44.02	-22.16	-55.26	-32.00	47.49
	Ge_{12a}^{2-}	Ge_{12b}^{2-}	Ge_{12c}^{2-}	Ge_{12d}^{2-}	
Structure	Icos	TTP	TTP	TTP	
Symmetry	$C_1(I_h0.1)$	C_1	C_1	C_{2v}	
ΔE [PBEPBE/6-311+G(<i>d</i>)] _{ZPE}	0.000	0.067	0.329	0.322	
ΔE [MP2/6-31+G(<i>d</i>)]	0.873	0.000			
ΔE [CCSD(T)/6-31+G(<i>d</i>)]	0.000	0.038			
HOMO-LUMO gap ^b	2.038	1.293	0.846	1.442	
NICS ^b	11.78	-43.77	-40.50	-20.99	
	Sn_{12a}^{2-}	Sn_{12b}^{2-}			
Structure	Icos	TTP			
Symmetry	$C_1(I_h0.01)$	C_1			
ΔE [PBEPBE/LANL2DZ] _{ZPE}	0.000	0.748			
HOMO-LUMO gap ^b	1.870	0.676			
NICS ^b	2.62	-29.70			

^aSymmetry is obtained within a numerical tolerance of 0.001 Å and is based on geometries optimized at PBEPBE/6-311+G(*d*) level for (Si and Ge) and PBEPBE/LANL2DZ (for Sn) level. Higher symmetries with larger tolerance are assigned in parentheses.

^bHOMO-LUMO gaps and NICS values are calculated at PBEPBE/6-311+G(*d*) level and PBEPBE/LANL2DZ level (for Sn).

clusters.¹⁵ The DFT-BH search provides a compromise between computing time and sufficient accuracy in structural determination and total-energy calculation.

Next, among the 200–400 isomers for the Zintl dianion clusters, the top ten low-lying isomers are collected as candidates for the lowest-energy structure. For Si_{12}^{2-} and Ge_{12}^{2-} , those isomers with energy difference from the lowest-lying isomer less than 0.3 eV (Table I) are further reoptimized using an all-electron DFT method (PBEPBE functional) with the 6-311+G(*d*) diffuse basis set, as well as using the second-order Moller-Plesset perturbation¹⁶ (MP2) method with the 6-31+G(*d*) basis set. Both methods are implemented in GAUSSIAN03 package.¹⁷ Calculation of harmonic vibrational frequencies is also performed to make sure that the optimized structures give no imaginary frequencies. For Sn_{12}^{2-} , the PBEPBE/LANL2DZ functional/basis set is chosen for geometric optimization and frequency calculation. In addition, the nuclear NICS values are calculated using the gauge-independent atomic orbital (GIAO) method¹⁸ at PBEPBE/6-311+G(*d*) level for Si and Ge, and at PBEPBE/LANL2DZ level for Sn. The canonical MO (CMO) NICS values are also calculated for the low-lying isomers of Si and Ge using the NBO 5.0 program.¹⁹

Last, to determine the lowest-energy structure among top candidate isomers of Si and Ge obtained from step 2, the

single-point energy calculation using the coupled-cluster method with single, double, and perturbative triple excitations²⁰ [CCSD(T)] and with a larger and more diffusive 6-311+G(2*d*) basis set for Si and the same 6-31+G(*d*) basis set for Ge is performed, based on geometric structures optimized at the MP2/6-31+G(*d*) level of theory/basis set.

III. RESULTS AND DISCUSSIONS

In the step-1 BH search, the lowest-energy isomer of Si_{12}^{2-} was obtained within 200 Monte Carlo (MC) steps. Three independent initial structures were used. For Sn_{12}^{2-} , the lowest-energy isomers structure (stannaspherene) can be quickly achieved, typically within 100 MC steps and regardless of the initial structure. For Ge_{12}^{2-} , however, the lowest-energy structure is much harder to attain, largely because there are two competing lowest-energy isomers with very different structures (see Sec. III B below), one contains the tricapped trigonal prism (TTP) motif and the other is a *closo* cage, i.e., the icosahedral structure.

The top ten low-energy isomers obtained from step 1 are listed in Table I. The top four candidates of Si_{12}^{2-} , top two of Ge_{12}^{2-} , and Sn_{12}^{2-} are plotted in Fig. 1, where the TTP motif is highlighted in blue. For Si_{12}^{2-} and Ge_{12}^{2-} , zero-point energy correction at the MP2/6-31+G(*d*)

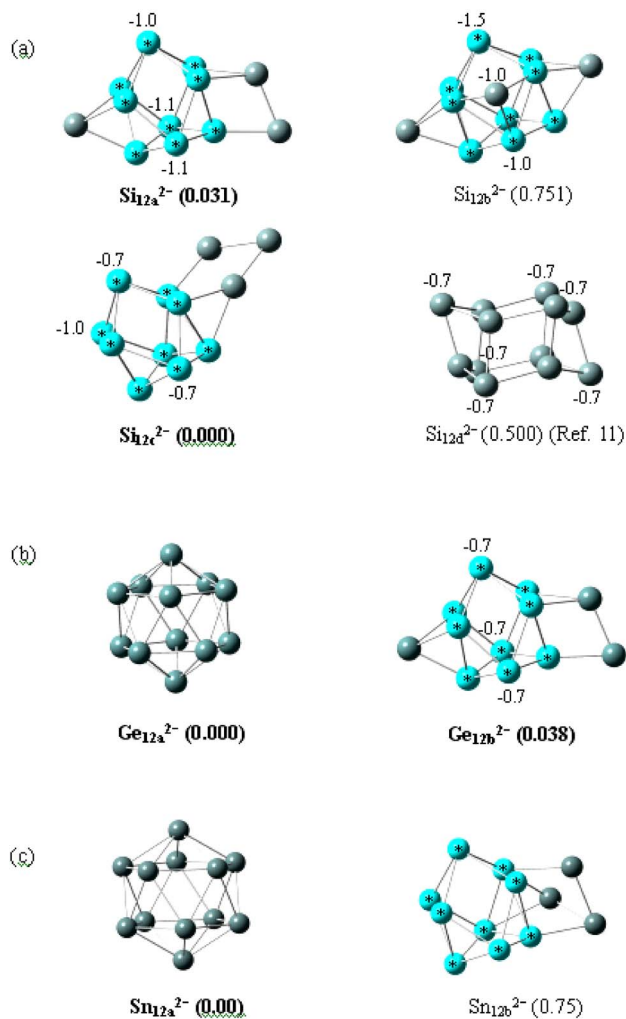


FIG. 1. (Color online) Optimized structures of low-lying Si_{12}^{2-} , Ge_{12}^{2-} , and Sn_{12}^{2-} isomers. Relative energies (in parentheses) are computed at CCSD(T)/6-311+G(2d)//MP2/6-31+G(d) level for Si_{12}^{2-} , CCSD(T)/6-31+G(d)//MP2/6-31+G(d) for Ge_{12}^{2-} , and at PBEPBE/LANL2DZ for Sn_{12}^{2-} . Energies are in units of eV. Lowest-energy structures are in bold index. Sn_{12b}^{2-} is the lowest-energy isomer that contains a TTP motif. The figure is prepared using GAUSSVIEW 3.0 program. The TTP motif is highlighted in blue with a star. Atoms with large negative Mulliken charge ($\leq -0.7e$) are also highlighted.

level of theory as well as the single-point energies calculated at the MP2/6-311+G(2d)//MP2/6-31+G(d) and CCSD(T)/6-311+G(2d)//MP2/6-31+G(d) levels of theory are given in Table II (see below for discussions). Also given in Table II are the gaps between the highest occupied MOs and the lowest unoccupied MOs (HOMO-LUMO gaps) and the NICS values, calculated at the PBEPBE/6-311+G(d) (for Si and Ge) and PBEPBE/LANL2DZ (for Sn) level of theory. The NICS value is an indicator of molecular aromaticity, which has been used to characterize relative stabilities among various Zintl $I_h\text{-E}_{12}^{2-}$ cluster with empty-cage structures.^{11,21} We have also calculated the NICS value at the center of TTP motif (Fig. 1). In addition, CMO analysis (implemented in the NBO 5.0 program)¹⁹ is carried out to evaluate the contribution of each molecular orbital to NICS value (Table III).

A. Si_{12}^{2-}

The TTP motif is known as one of major structural motifs in low-energy silicon clusters of $\text{Si}_{10}\text{-Si}_{20}$.²² Indeed, among the top ten low-lying isomers of Si_{12}^{2-} , six contain the TTP motif (highlighted in Table I). The top four low-lying isomers [Fig. 1(a)] have been reoptimized using MP2/6-31+G(d) level of theory. The MP2/6-31+G(d) calculations result in nearly the same geometries and the same energy ranking but with different energy difference compared to the DFT calculations. MP2 calculation with a larger diffuse basis set [MP2/6-311+G(2d)//MP2/6-31+G(d)] also shows that Si_{12a}^{2-} is the lowest-energy isomer as predicted based on the DFT calculation [Table II and Fig. 1(a)]. Note also that Si_{12a}^{2-} contains a TTP motif and has C_s symmetry. The second lowest-energy structure Si_{12b}^{2-} (at the DFT level) becomes the highest-energy isomer [at CCSD(T) level] among the top four isomers. Note also that Si_{12b} is the lowest-energy structure of neutral Si_{12} cluster.²²⁻²⁴ Si_{12c}^{2-} is the third lowest-energy isomer (at DFT level). However, it is nearly degenerate in energy [at CCSD(T) level] with Si_{12a}^{2-} and, thus, it is a competitive candidate for the lowest-energy isomer. The chair-shaped structure Si_{12d}^{2-} with D_{3d} symmetry¹¹ is the third lowest-energy structure at CCSD(T) level but it has the largest HOMO-LUMO gap of 1.9 eV. The two lowest-energy isomers Si_{12a}^{2-} and Si_{12c}^{2-} also have sizable HOMO-LUMO gaps (1.3 and 1.5 eV, respectively).

Both Si_{12a}^{2-} and Si_{12c}^{2-} exhibit large negative NICS values (-44.0 and -55.3 ppm, respectively), suggesting that the lowest-energy isomers are aromatic. The total NICS value stems mainly from valence MOs, based on the CMO-NICS analysis (Table III). The least valence-orbital contribution to the total NICS value is 90.6% for Si_{12b}^{2-} . Note that the TTP cluster Si_9^{2-} itself entails a large negative NICS value (-37.5 ppm) at its center [based on PBEPBE/6-311+G(d) calculation]. Hence, Zintl dianion cluster Si_{12}^{2-} which contains a TTP motif is expected to show strong aromaticity. The CMO-NICS analysis suggests that the positive CMO-NICS values are due to the chemical bonds associated with the three non-TTP atoms, rather than the bonds associated within the TTP structure. Atoms with the Mulliken charge $\leq -0.7e$ are shown in Fig. 1. Most of these atoms belong to the TTP motif. For the chair-shaped Si_{12d}^{2-} , large negative charges accumulate on six atoms [see Fig. 1(a)]. From Si to Ge and to Sn, the charge distribution on the TTP-containing clusters becomes more uniform.

For the purpose of comparison, we included data for the empty-cage icosahedral isomer $I_h\text{-Si}_{12}^{2-}$ in Table II. Unlike the stannaspherene $I_h\text{-Sn}_{12}^{2-}$ and plumbaspherene $I_h\text{-Pb}_{12}^{2-}$, which are the lowest-energy structures for Sn_{12}^{2-} and Pb_{12}^{2-} , respectively, the $I_h\text{-Si}_{12}^{2-}$ has a much higher energy than Si_{12a}^{2-} and Si_{12c}^{2-} (>1 eV at DFT level). In addition, consistent with the results of both King *et al.* and Zdzetsis, we found that $I_h\text{-Si}_{12}^{2-}$ entails a large positive NICS value (47.5 ppm), indicating strong antiaromatic character. Hence, the $I_h\text{-Si}_{12}^{2-}$ isomer is unlikely to exist in the cluster beam.^{5,6,11} The natural bond orbital (NBO)-CMO analysis shows that the Zintl dianion with I_h symmetry has only one-center core or one-center lone-pair type of MOs. The five-

TABLE III. CMO-NICS values of low-lying Zintl dianions. The calculations are performed at PBE/PBE/6-311+G(*d*) level (for Si and Ge) and PBE/PBE/LANL2DZ level (for Sn). Positive (total) NICS values are highlighted by **bold**.

CMO	Si_{12a}^{2-}	Si_{12b}^{2-}	Si_{12c}^{2-}	Si_{12d}^{2-}	$I_h\text{-Si}_{12}^{2-}$	CMO	Ge_{12a}^{2-}	Ge_{12b}^{2-}	Sn_{12a}^{2-}	Sn_{12b}^{2-}
61	-10.46	-9.44	-8.87	-8.11	-8.72	169	-8.04	-9.29	-7.19	-6.26
62	-13.14	-13.21	-9.69	-7.69	-14.52	170	-10.53	-8.60	-7.7	-8.07
63	-3.17	-8.54	-7.34	-7.70	-14.76	171	-10.52	-6.46	-7.7	-6.72
64	-2.12	-6.97	-8.56	-4.80	-14.78	172	-10.50	-8.05	-7.7	-6.90
65	-10.01	-12.54	-7.14	-8.45	-6.15	173	-5.12	-5.75	-3.89	-5.03
66	-5.42	-7.73	-2.83	-8.46	-6.15	174	-5.12	-4.70	-3.89	-3.29
67	-0.47	-0.64	-5.98	-0.80	-6.15	175	-5.12	-4.20	-3.89	-3.04
68	-3.62	-2.91	-1.62	-0.82	-6.14	176	-5.11	-4.24	-3.89	-2.82
69	-4.18	-2.21	-5.25	-0.67	-6.15	177	-5.11	-4.13	-3.89	-2.80
70	-2.28	1.00	-5.57	-0.29	1.67	178	-1.75	-4.03	-0.83	-2.81
71	-3.19	1.88	-0.07	-0.28	1.67	179	-1.76	-2.61	-0.83	-2.13
72	-1.57	1.55	-1.99	-6.32	1.67	180	-1.75	-2.78	-0.83	-1.63
73	-5.14	-4.95	-6.76	-7.27	-10.53	181	-7.88	-6.38	-6.14	-4.29
74	-6.34	-6.34	-4.01	-5.77	-10.53	182	-8.42	-6.42	-6.14	-2.77
75	-3.37	-4.00	-0.05	-4.81	-10.53	183	-8.42	-4.09	-6.14	-2.34
76	-2.29	-2.20	-0.13	-4.80	-10.53	184	-8.42	-4.11	-6.14	-2.02
77	-0.35	-4.72	-2.14	1.80	-8.13	185	-8.41	-3.53	-6.32	-2.38
78	-0.73	-2.99	-3.56	1.81	2.68	186	1.61	-0.38	1.19	-1.43
79	0.68	-6.35	-2.08	6.61	2.17	187	1.54	3.19	1.19	1.02
80	-1.01	-0.26	0.56	6.61	2.16	188	1.68	0.17	1.2	2.78
81	0.67	2.18	0.27	-2.76	34.44	189	24.58	6.40	16.38	5.45
82	-2.06	13.98	3.12	11.32	34.44	190	24.60	3.80	16.43	4.07
83	11.13	19.54	6.36	-1.96	34.44	191	24.63	10.66	16.43	5.13
84	11.31	15.48	10.46	11.88	34.43	192	24.75	8.74	16.44	10.27
85	14.75	20.31	9.47	11.89	34.43	193	24.75	17.85	16.46	8.32
Total ^a	-44.02	-22.16	-55.26	-32.00	47.49	Total	11.78	-43.77	2.62	-29.70
Val.% ^b	96.41	90.61	96.63	93.25	106.19	Val.%	137.18	88.97	99.62	99.97

^aSum of CMO-NICS values for valence electrons.^bPercent of the contribution of valence electrons to the total NICS value.

fold degenerate HOMO is composed of localized lone-pair NBOs which contribute 92.0% of the total positive NICS value for $I_h\text{-Si}_{12}^{2-}$.

The relative stabilities of the four low-lying isomers of Si_{12}^{2-} at higher temperatures can be studied from Gibbs free energy versus temperature calculation [Fig. 2(a)]. It appears that Si_{12b}^{2-} , the lowest-energy isomer of neutral cluster, could become increasingly stable than Si_{12a}^{2-} as the temperature is increased. Although the Gibbs free energy calculation is based on harmonic approximation which may be inaccurate at high temperatures, we expect that the trend in relative stabilities at room temperature is still qualitatively correct.

It should be noted that the intraligands (or metal dopant) might be able to stabilize certain cage clusters, such as the icosahedral Si_{12}^{2-} . In our calculation at PBE/ECP level, we found that the optimized endohedral $\text{Pb}@I_h\text{-Si}_{12}^{2-}$ has a lower electronic energy than the exohedral PbSi_{12a}^{2-} by 0.51 eV. The endohedral $\text{Pb}@I_h\text{-Si}_{12}^{2-}$ also has a larger HOMO-LUMO gap of 1.58 eV than 0.88 eV of PbSi_{12a}^{2-} .

Last, to compare the MOs of $I_h\text{-Si}_{12}^{2-}$ with those of the TTP Si_{12}^{2-} , energy levels of twenty-five valence MOs of Si_{12a}^{2-} , Si_{12c}^{2-} , and $I_h\text{-Si}_{12}^{2-}$, calculated at PBE/PBE/6-311+G(*d*) level, are schematically plotted in Fig. 3. It can be seen that the TTP Si_{12}^{2-} has smaller $3s^2$ and $3p$ gaps than $I_h\text{-Si}_{12}^{2-}$, indicating that the inner $3s$ orbitals are more delocalized.

B. Ge_{12}^{2-}

Among the top ten low-lying isomers shown in Table I, six isomers contain the TTP motif. At the DFT level of theory, Ge_{12a}^{2-} is the lowest-energy isomer, while at the MP2 level, Ge_{12b}^{2-} is the lowest-energy isomer. At higher level CCSD(T)/6-31+G(*d*)/MP2/6-31+G(*d*) calculation, Ge_{12a}^{2-} and Ge_{12b}^{2-} are almost degenerate in energy. Hence, both can be viewed as candidates for the lowest-energy structure. Ge_{12b}^{2-} contains a TTP motif and exhibits the same structure as Si_{12a}^{2-} , which is the lowest-energy structure of Si_{12}^{2-} . Ge_{2c}^{2-} also contains a TTP motif and exhibits the same structure as Sn_{12b}^{2-} . The fourth lowest-lying structure Ge_{12d}^{2-} has C_{2v} symmetry and is the lowest-energy structure of neutral Ge_{12} cluster.^{24,25} Ge_{12a}^{2-} exhibits the icosahedral structure, similar to the stannaspherene $I_h\text{-Sn}_{12}^{2-}$ and plum-baspherene $I_h\text{-Pb}_{12}^{2-}$. Thus, Ge_{12a}^{2-} may be named as *germaniaspherene*.

The valence MOs of Ge_{12a}^{2-} are very similar to those of $I_h\text{-Sn}_{12a}^{2-}$ and $I_h\text{-Pb}_{12}^{2-}$, which include four delocalized π bonding orbitals (a_g and t_{1u}) and nine σ bonding orbitals (g_u and h_g)^{5,6} and twelve localized $4s$ orbitals (see Fig. 3). Note that for $I_h\text{-Pb}_{12}^{2-}$, the five degenerated σ -bonding h_g orbitals have higher electronic energy than π -bonding t_{1u} orbitals, but the energy ordering is reversed for Ge_{12a}^{2-} and $I_h\text{-Sn}_{12}^{2-}$.

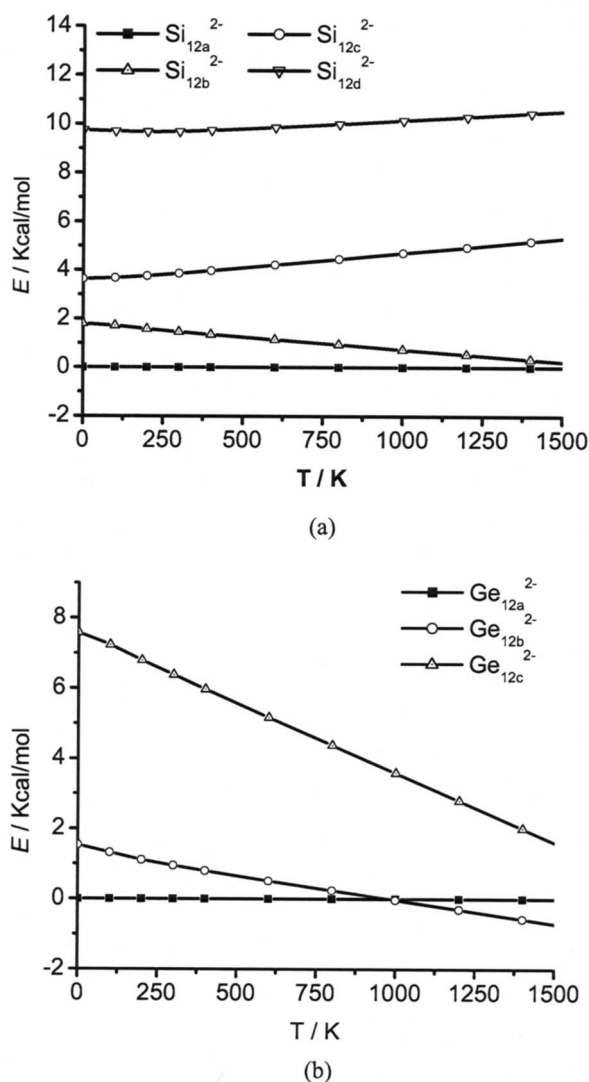


FIG. 2. Relative Gibbs free energy vs temperature for (a) Si_{12a}^{2-} (■, 0 eV line), Si_{12b}^{2-} (△), Si_{12c}^{2-} (○), and Si_{12d}^{2-} (▽); and (b) Ge_{12a}^{2-} (■, 0 eV line), Ge_{12b}^{2-} (○), and Ge_{12c}^{2-} (△). The calculations are carried out at PBE/PBE/6-311+G(*d*) level.

The energy gap between g_u and h_g orbitals increases from $I_h\text{-Sn}_{12}^{2-}$ (1.3 eV) to Ge_{12a}^{2-} (1.8 eV) and to $I_h\text{-Sn}_{12}^{2-}$ (2.6 eV). In Fig. 4, it can be seen that the HOMO of Ge_{12a}^{2-} is slightly more delocalized compared to $I_h\text{-Sn}_{12a}^{2-}$ and $I_h\text{-Si}_{12}^{2-}$.

Ge_{12b}^{2-} is another candidate for the lowest-energy structure. It exhibits a large negative NICS (−43.8 ppm) at the center of TTP structure, due to relatively less paramagnetic contributions of its five highest occupied orbitals (Table III). Similar to TTP Si_9^{2-} , the TTP Ge_9^{2-} unit itself also entails a large negative NICS value [−44.5 ppm calculated at PBE/PBE/6-311+G(*d*) level]. Hence, all TTP-containing dianions are expected to show aromatic character. Moreover, similar to Si_{12a}^{2-} , Ge_{12b}^{2-} also shows negative charges on the three capping atoms of TTP [Fig. 1(b)]. However, the magnitude of the charges is smaller compared to that of Si_{12a}^{2-} [Fig. 1(a)]. In Fig. 2(b), the Gibbs free energy versus temperature curves are shown. As the temperature is increased, Ge_{12b}^{2-} becomes increasingly stable than Ge_{12a}^{2-} . This is

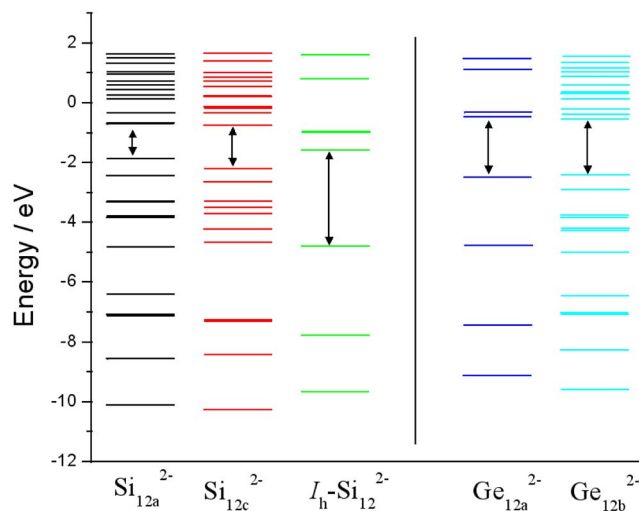


FIG. 3. (Color online) Energy levels of twenty-five valence molecular orbitals of Si_{12a}^{2-} , Si_{12c}^{2-} , and $I_h\text{-Si}_{12}^{2-}$, calculated at PBE/PBE/6-311+G(*d*) level. MOs of Ge_{12a}^{2-} and Ge_{12b}^{2-} are also plotted. The arrows separate the inner ($3s^2$ or $4s^2$) from the outer valence orbitals ($3p$ or $4p$).

another factor that favors Ge_{12b}^{2-} over Ge_{12a}^{2-} as the most stable dianion cluster in the gas phase, in addition to the total NICS factor.

Figure 4 shows a higher delocalized HOMO of Ge_{12a}^{2-} compared to two other icosahedral cages $I_h\text{-Si}_{12}^{2-}$ and Sn_{12a}^{2-} . This is likely due to the greater contribution of s electrons to the HOMO, which is 49.4%, calculated at PBE/PBE/6-311+G(*d*) level of theory. As a comparison, the contributions of s electrons to the HOMO are $\sim 43\%$ for $I_h\text{-Si}_{12}^{2-}$ and 38.9% for Sn_{12a}^{2-} . Ge_{12b}^{2-} and Si_{12a}^{2-} exhibit the same structure, as well as the same patterns of MOs (see Fig. 4). In Fig. 3, energy levels of MOs of Ge_{12a}^{2-} and Ge_{12b}^{2-} are also plotted. It can be seen that the TTP Ge_{12b}^{2-} shows similar $4s^2$ localization as the $I_h\text{-Ge}_{12a}^{2-}$.

C. Sn_{12}^{2-}

The BH search shows that the stannaspherene Sn_{12a}^{2-} [Fig. 1(c)] is unequivocally the lowest-energy isomer. The next lowest-energy TTP-containing isomer Sn_{12b}^{2-} is 0.54 eV higher in energy (at PBE/DNP-ECP level) or 0.75 eV higher in energy (at PBE/PBE/LANL2DZ level) than Sn_{12a}^{2-} . It is worth noting that Sn_{12b}^{2-} exhibits the same structure as the third lowest-lying structure Ge_{12c}^{2-} and the fifth lowest-lying structure Si_{12e}^{2-} (Table I). Expectedly, the TTP-containing isomer Sn_{12b}^{2-} has a large negative NICS value of −29.7 ppm. Although Sn_{12a}^{2-} has a positive NICS value (2.6 ppm), this value is much smaller than NICS values of $I_h\text{-Si}_{12}^{2-}$ (47.5 ppm) and Ge_{12a}^{2-} (11.8 ppm).

We note that the lowest-energy structure of neutral Sn_{12} contains a TTP motif,²⁴ whereas the lowest-energy structure of *monoanion* Sn_{12}^- is an empty cage with C_{5v} symmetry.⁵ Analysis of the valence MOs of Sn_{12a}^{2-} has been reported in a previous joint experimental/theoretical study.⁵ Sn_{12a}^{2-} exhibits similar MOs as $I_h\text{-Ge}_{12a}^{2-}$ and $I_h\text{-Sn}_{12}^{2-}$ (Fig. 4).

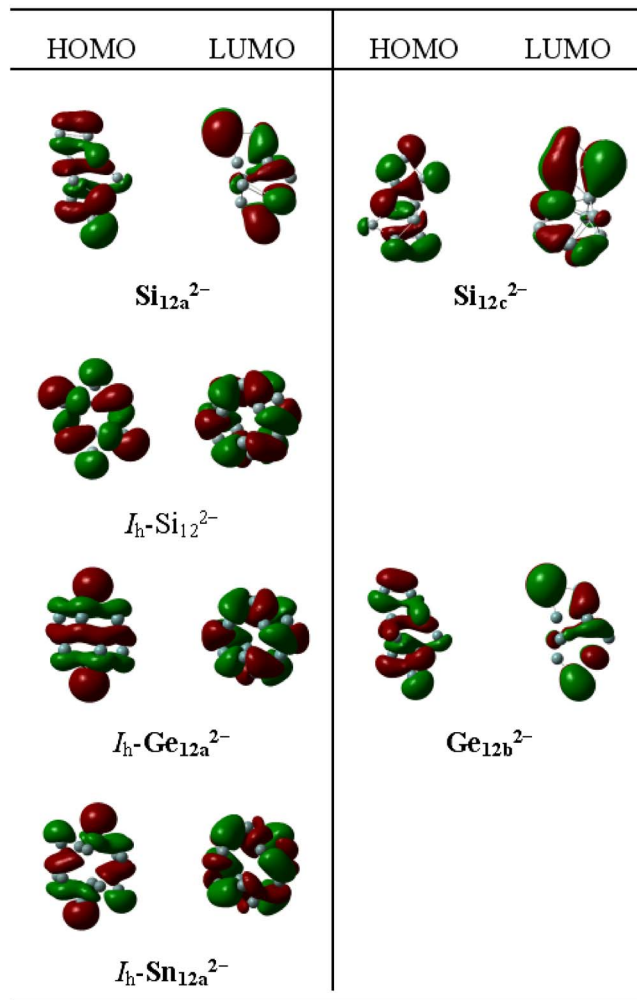


FIG. 4. (Color online) HOMO and LUMO of the low-lying isomers. The structures are optimized at PBEPBE/6-311+G(d) level for Si_{12}^{2-} and Ge_{12}^{2-} , and PBEPBE/LANL2DZ for Sn_{12}^{2-} .

IV. CONCLUSIONS

We perform a global-minimum search for the lowest-energy structures of Zintl dianions Si_{12}^{2-} , Ge_{12}^{2-} , and Sn_{12}^{2-} , by using the basin-hopping global optimization method combined with density functional theory geometric optimization. High-level *ab initio* methods are used to determine relative stabilities and energy ranking among candidate low-lying isomers of the dianions. For the first time, two candidates of the lowest-energy structures of Si_{12}^{2-} are reported, namely, Si_{12a}^{2-} and Si_{12c}^{2-} . Both candidate isomers contain a TTP motif and both have C_s symmetry. Unlike other group-14 elements, the icosahedral isomer $I_h\text{-Si}_{12}^{2-}$ is much higher in energy compared to top ten low-lying isomers of Si_{12}^{2-} .

For Ge_{12}^{2-} , two candidates for the lowest-energy structure are identified through the BH search, namely, $I_h\text{-Ge}_{12a}^{2-}$ and a TTP-containing isomer Ge_{12b}^{2-} . The latter exhibits the same structure as Si_{12a}^{2-} , whereas the former, germaniaspherene, exhibits the same structure as the stannaspherene $I_h\text{-Sn}_{12a}^{2-}$. As expected, the structural characteristics of germaniaspherene are somewhere in between those of silicon and tin clusters. On the relative stability between $I_h\text{-Ge}_{12a}^{2-}$ and Ge_{12b}^{2-} , Ge_{12a}^{2-} entails a much larger

HOMO-LUMO gap (2.04 eV) than Ge_{12b}^{2-} (1.29 eV) while Ge_{12b}^{2-} has a lower free energy than $I_h\text{-Ge}_{12a}^{2-}$ at high temperature. Moreover, the Ge_{12b}^{2-} entails a large negative NICS value (~ -44) at the center of TTP, indicating strongly aromatic character. Hence, freestanding Ge_{12b}^{2-} may be more likely to exist in the cluster beam than the germaniaspherene Ge_{12a}^{2-} .

Finally, for Sn_{12}^{2-} , the global search confirms a previous finding that the lowest-energy structure is an empty cage with icosahedral structure (stannaspherene). Although the stannaspherene has a positive NICS value (2.6 ppm) at the center of the cage, this value is much smaller than that of $I_h\text{-Si}_{12}^{2-}$ (47.5 ppm) and that of germaniaspherene (11.8 ppm), indicating that the stannaspherene is marginally antiaromatic. In general, a strongly antiaromatic Zintl cage is expected to be unstable, as demonstrated in the case of Si_{12}^{2-} (Ref. 11). However, the stannaspherene Sn_{12}^{2-} which has been found to be very stable in the gas phase³ is an exception. This result suggests that having strong aromaticity is perhaps only sufficient but not necessary to construct highly stable Zintl dianion polyhedrons.

ACKNOWLEDGMENTS

This research was supported in part by grants from the DOE (No. DE-FG02-04ER46164), NSF (CHE and CMMI), and the Nebraska Research Initiative, and by the Research Computing Facility at the University of Nebraska-Lincoln.

- A. Spiekermann, S. D. Hoffmann, and T. F. Fässler, *Angew. Chem., Int. Ed.* **45**, 3459 (2006); D. Y. Zubarev, A. N. Alexandrova, A. I. Boldyrev, L. F. Cui, X. Li, L. S. Wang, *J. Chem. Phys.* **124**, 124305 (2006).
- R. B. King, T. Heine, C. Corminboeuf, and P. v. R. Schleyer, *J. Am. Chem. Soc.* **126**, 430 (2003).
- A. D. Zdzetsis, *J. Chem. Phys.* **127**, 014314 (2007); 244308 (2007).
- K. Wade, *Adv. Inorg. Chem. Radiochem.* **18**, 1 (1976).
- L. F. Cui, X. Huang, L. M. Wang, D. Y. Zubarev, A. I. Boldyrev, J. Li, and L. S. Wang, *J. Am. Chem. Soc.* **128**, 8390 (2006).
- L. F. Cui, X. Huang, L. M. Wang, J. Li, and L. S. Wang, *J. Phys. Chem. A* **110**, 10169 (2006).
- E. N. Esenturk, J. Fettinger, and B. Eichhorn, *J. Am. Chem. Soc.* **128**, 9178 (2006).
- E. N. Esenturk, J. Fettinger, Y. F. Lam, and B. Eichhorn, *Angew. Chem., Int. Ed.* **43**, 2132 (2004).
- L. F. Cui, X. Huang, L. M. Wang, J. Li, and L. S. Wang, *Angew. Chem., Int. Ed.* **46**, 742 (2007).
- S. Neukermans, E. Janssens, Z. F. Chen, R. E. Silverans, P. v. R. Schleyer, and P. Lievens, *Phys. Rev. Lett.* **92**, 163401 (2004).
- Z. F. Chen, S. Neukermans, X. Wang, E. Janssens, Z. Zhou, R. E. Silverans, R. B. King, P. v. R. Schleyer, and P. Lievens, *J. Am. Chem. Soc.* **128**, 12829 (2006).
- D. J. Wales, *Energy Landscapes: With Applications to Clusters, Biomolecules and Glasses* (Cambridge University, Cambridge, 2003).
- J. P. Perdew, K. Burke, and M. Ernzerhof, *Phys. Rev. Lett.* **77**, 3865 (1996); **78**, 1396 (1997).
- B. Delley, *J. Chem. Phys.* **92**, 508 (1990); **113**, 7756 (2000).
- B. Kiran, S. Bulusu, H. J. Zhai, S. Yoo, X. C. Zeng, and L. S. Wang, *Proc. Natl. Acad. Sci. U.S.A.* **102**, 961 (2005); S. Bulusu, S. Yoo, and X. C. Zeng, *J. Chem. Phys.* **122**, 184325 (2005); S. Bulusu, X. Li, L. S. Wang, and X. C. Zeng, *Proc. Natl. Acad. Sci. U.S.A.* **103**, 8326 (2006).
- C. Moller and M. S. Plesset, *Phys. Rev.* **46**, 618 (1934); M. Head-Gordon, J. A. Pople, and M. J. Frisch, *Chem. Phys. Lett.* **153**, 503 (1988); J. B. Foresman and A. Frisch, *Exploring Chemistry with Electronic Structure Methods*, 2nd ed. (Gaussian, Pittsburgh, PA, 1996).
- M. J. Frisch, G. W. Trucks, H. B. Schlegel *et al.*, GAUSSVIEW 3.0, Gaussian, Inc., Pittsburgh, PA, 2002.
- R. Ditchfield, *Mol. Phys.* **27**, 789 (1974); K. Wolinski, J. F. Hinton, and

- P. Pulay, *J. Am. Chem. Soc.* **112**, 8251 (1990).
- ¹⁹J. A. Bohmann, F. Weinhold, T. C. Tarrar, *J. Chem. Phys.* **107**, 1173 (1997); E. D. Glendening, J. K. Badenhop, A. E. Reed, J. E. Carpenter, J. A. Bohmann, C. M. Morales, and F. Weinhold, NBO 5.0, Theoretical Chemistry Institute, University of Wisconsin, Madison, WI, 2001 (<http://www.chem.wisc.edu/~nbo5>).
- ²⁰J. A. Pople, R. Krishnan, H. B. Schlegel, and J. S. Binkley, *Int. J. Quantum Chem.* **14**, 545 (1978); K. Raghavachari, G. W. Trucks, M. Head-Gordon, and J. A. Pople, *Chem. Phys. Lett.* **157**, 479 (1989).
- ²¹D. L. Chen, W. Q. Tian, J. K. Feng, and C. C. Sun, *J. Phys. Chem. A* **111**, 8277 (2007).
- ²²K. M. Ho, A. A. Shvartsburg, B. Pan, Z. Y. Lu, C. Z. Wang, J. G. Wacker, J. L. Fye, and M. F. Jarrold, *Nature (London)* **392**, 582 (1998); X. L. Zhu, X. C. Zeng, Y. A. Lei, and B. Pan, *J. Chem. Phys.* **120**, 8985 (2004); S. Yoo and X. C. Zeng, *J. Chem. Phys.* **123**, 164303 (2005).
- ²³A. Tekin and B. Hartke, *Phys. Chem. Chem. Phys.* **6**, 503 (2004).
- ²⁴Z. Y. Lu, C. Z. Zhuang, and K. M. Ho, *Phys. Rev. B* **61**, 2329 (2000).
- ²⁵S. Bulusu, S. Yoo, and X. C. Zeng, *J. Chem. Phys.* **122**, 164305 (2005).